Fibrin-bound thrombin determines clot structure and blood thrombogenicity in normofibrinogenemia and dysfibrinogenemia

Siyu Sun,[1] Mark Roest,[1] Rolf T. Urbanus,[2] Elena Campello,[3] Sarah Beck,[4] Cristiana Bulato,[3] Simon D. Connell,[5] Philip G. de Groot,[1] Timea Feller,[6] Dana Huskens,[1] Joke Konings,[1] Rita Marchi,[7] Harmen Middelveld,[1] Patricia Öftering,[4] Bernhard Nieswandt,[4] Alessandro Casini,[7] Robert A. S. Ariëns,[6] Paolo Simioni,[3] Johan W. M. Heemskerk[1] and Bas de Laat[1]

[1]Synapse Research Institute Maastricht, Maastricht, the Netherlands; [2]Van Kreveldkliniek, University Medical Center Utrecht, the Netherlands; [3]Department of Medicine, University of Padua, Padova, Italy; [4]Rudolf Virchow Center for Integrative and Translational Bioimaging and Institute of Experimental Biomedicine, Julius-Maximilians-Universität Würzburg, Würzburg, Germany; [5]Molecular and Nanoscale Physics Group, School of Physics, University of Leeds, Leeds, UK; [6]Discovery and Translational Science Department, Leeds Institute of Cardiovascular and Metabolic Medicine, University of Leeds, Leeds, UK and [7]Division of Angiology and Hemostasis, Department of Medicine, University Hospitals of Geneva, University of Geneva, Geneva, Switzerland

Correspondence: M. Roest
M.Roest@thrombin.org

Received: July 1, 2025.
Accepted: January 26, 2026.
Early view: February 5, 2026.

https://doi.org/10.3324/haematol.2025.288585

SUPPLEMENT

Fibrin-bound thrombin determines clot structure and blood thrombogenicity in normofibrinogenemia and dysfibrinogenemia

Siyu Sun[1], Mark Roest[1*], Rolf T. Urbanus[2], Elena Campello[3], Sarah Beck[4], Cristiana Bulato[3], Simon D. Connell[5], Philip G. de Groot[1], Timea Feller[6], Dana Huskens[1], Joke Konings[1], Rita Marchi[7], Harmen Middelveld[1], Patricia Öftering[4], Bernhard Nieswandt[4], Alessandro Casini[7], Robert A. S. Ariëns[6], Paolo Simioni[3], Johan W. M. Heemskerk[1], Bas de Laat[1]

[1]Synapse Research Institute Maastricht, Kon. Emmaplein 7, 6217 KD, Maastricht, The Netherlands; [2]Van Kreveldkliniek, University Medical Centre Utrecht, The Netherlands; [3]Department of Medicine, University of Padua, Padova, Italy; [4]Rudolf Virchow Center for Integrative and Translational Bioimaging & Institute of Experimental Biomedicine, Julius-Maximilians-Universität Würzburg, Germany; [5]Molecular and Nanoscale Physics Group, School of Physics, University of Leeds, Leeds, UK; [6]Discovery and Translational Science Department, Leeds Institute of Cardiovascular and Metabolic Medicine, University of Leeds, Leeds, UK; [7]Division of Angiology and Hemostasis, Department of Medicine, University Hospitals of Geneva, University of Geneva, Switzerland.

Supplemental Methods

Chemicals

Recombinant tissue factor (TF, Innovin) was purchased from Siemens Healthineers (Marburg, Germany); fluorogenic substrate Z-Gly-Gly-Arg-aminomethyl coumarin (ZGGR-AMC) and peptide GPRP from Bachem (Bubendorf, Switzerland). Thrombin calibrator (α2-macroglobulin-thrombin complex), human thrombin, protease III and activated protein C were prepared in-house by Synapse Research Institute (Maastricht, The Netherlands).[1,2] Synthetic phospholipid mixture consisting of 20 mol% phosphatidylserine, 20 mol% phosphatidylethanolamine and 60 mol% phosphatidylcholine was from Avanti Polar Lipids (Alabaster, AL, USA). Alexa Fluor-647 anti-glycoprotein IX antibody (56F8) and Alexa Fluor-488 fibrinogen were purchased from Invitrogen Life Technologies (Budapest, Hungary). Purified ancrod was from Knoll (Ludwigshafen, Germany); chromogenic substrate S2238 from Chromogenix (Brussels, Belgium). Staphylocoagulase was purified in house, as described by Hendrix et al.[3] Echis carinatus venom was obtained from Sigma-Aldrich (Darmstadt, Germany). Obtained from Invitrogen Life Technologies (Burlington, Canada) were thrombin exosite 1 and 2-directed DNA aptamers, Apt1 (GGTTGGTGTGGTTGG, HD1) and Apt2 (AGTCCGTGGTGGTAGGGCAGGTTGGGGTGACT, HD22), and the exosite 1-2-directed aptamer Apt3 (combined HD1 and HD22: GGTTGGTGTGGTTGG-AAAAAAAAAAAAAAA-AGTCCGTGGTGGTAGGGCAGGTTGGGGTGACT). The FGA/FGB-derived peptides, Pep1 (SACKDSDWPFCSDEDWNYKC) and Pep2 (YRARPAKAAATQKKVERKAPDAGGCLHADPDLGVL), were chemically synthetized by Synpeptide (Nanjing, Jiangsu, China). Cross-linked collagen-related peptide (CRP-XL), as a platelet GPVI) agonist, came from CambCol (Cambridge, United Kingdom), and direct oral anticoagulant dabigatran was from Alsachim (Illkirch-Graffenstaden, France).

Normal pool plasma (NPP) was prepared in house.[4] Antithrombin-deficient plasma came from Hematologic Technologies (Essex Junction, VT, USA). Plasmas deficient in fibrinogen, factor IX, XI or XII were bought from Affinity Biologicals (Ancaster, Canada). A purified preparation of fibrinogen γ' was used, as described before.[5]

Antibodies

The single chain antibody Nb106 was generated in-house from a llama injected with fibrin degradation products, enriched in fibrin D-D and D-E-D dimers, according to described

procedures.[6,7] It was selected for binding to human fibrin monomers but not un-cleaved fibrinogen. The non-responsive single chain antibody Nb-Syn1C6 was raised similarly. Single chain antibody against human antithrombin was obtained from Biointron Biological (Shanghai, China).

Human blood donors and blood sample preparations

Studies with blood from healthy donors were approved by the Medical Ethical Committee of Maastricht University Medical Centre (NL31480.068.10). Patient studies were approved by the Research and Ethics Committees of Padua University Hospital Italy (protocol code 4303/AO17, July 28, 2017) and of the University Hospitals of Geneva (Switzerland). Studies were conducted in accordance with the Declaration of Helsinki. Blood donors had not taken anticoagulant or antiplatelet medication for at least two weeks, and gave written informed consent. Congenital dysfibrinogenemia was classified from a reduced fibrinogen activity level in comparison to the antigen level. Genotyping followed the International Society of Thrombosis and Haemostasis classification.[8] Screenings for *FGA*, *FGB* and *FGG* mutations were based on suspected dysfibrinogenemia, and were performed by PCR amplification of fibrinogen coding sequences, followed by Sanger sequencing.[9] Mutations were annotated as described in the Human Genome Variation Society guidelines. Gene nucleotide numbering was according to NIH GenBank sequences.

All human blood samples (9 volumes) were taken from the antecubital vein and were drawn into aseptic vacutainer tubes (Greiner Bio-One, Alphen a/d Rijn, The Netherlands), containing 3.2% sodium citrate (1 volume). The samples kept at room temperature were used within 2-3 h for experiments or plasma preparation. Routinely, blood cell parameters were measured with a cell counter analyser (SthemA 601, Stago, France). Platelet counts in the healthy subjects were within the normal range (150-400 × 10^9/L).

Platelet-rich plasma (PRP) and washed platelets were prepared, as outlined before.[2,10] In brief, PRP was obtained by centrifuging blood for 15 minutes at 250 g. For collecting washed platelets, PRP was supplemented with 10 vol% ACD medium (80 mM trisodium citrate, 52 mM citric acid and 180 mM glucose), after which the cells were spin down in 2 mL Eppendorf tubes at 1700 g for 2 minutes. After plasma removal, pellets were resuspended into 1 mL of Hepes buffer pH 6.6 (136 mM NaCl, 5 mM Hepes, 2.7 mM KCl, 2 mM $MgCl_2$, apyrase at 0.2 unit ADPase/mL, 0.1% glucose and 0.1% bovine serum albumin). After another addition of ACD, the tubes were recentrifuged. Washed platelets were resuspended per tube into 1 mL Hepes

buffer pH 7.45 (10 mM Hepes, 136 mM NaCl, 2.7 mM KCl, 2 mM $MgCl_2$, 0.1% glucose, and 0.1% bovine serum albumin).

Citrated blood samples, collected by venipuncture, from control subjects and patients were subjected to double centrifugation at 2000 g for 15 minutes at room temperature. Within 2 hours after blood sampling, plasmas were aliquoted and stored as at −80 °C until use. For cohort testing, plasmas were obtained from 64 healthy individuals, as described.[11] Included were samples from 28 males and 36 females, with mean ages of 34 and 32, respectively.

Mouse blood

Adult wildtype C57BL/6 mice (males and females) were maintained under specific pathogen-free conditions, as described before.[12] Experiments were performed in accordance with German law, and permission was obtained from the Animal Experimental Ethics Committee from the District of Lower Franconia (Germany). Mouse blood was obtained by orbital puncture, and collected into citrate anticoagulant.[12,13] Whole blood samples were used for microfluidic testing or for plasma preparation, as detailed elsewhere.[14]

Thrombin generation assessment

Using a 96-well-plate based method of calibrated thrombin generation (37 °C), the formation and ensuing inactivation of thrombin was monitored in centrifuged plasma or PRP samples, employing a low-affinity fluorogenic substrate for thrombin, which does not interfere with the coagulation process.[10,15] In brief, wells contained 80 µL plasma or PRP plus 20 µL of trigger solution: 1 pM TF and 4 µM procoagulant phospholipids, dissolved into BSA5 buffer (20 mM Hepes, 140 mM NaCl, 5 mg/mL bovine serum albumin, pH 7.35). In experiments with PRP, phospholipids were left out, as platelets provided the procoagulant membranes. Coagulation was started by dispensing 20 µL of substrate solution, consisting of 11 mM $CaCl_2$, 5.5 mM $MgCl_2$ and 417 µM Z-GGR-AMC, dissolved into BSA60 buffer (20 mM Hepes, 140 mM NaCl, 60 mg/mL BSA, pH 7.35). For each plasma type, additional wells were used, in which the trigger solution was replaced by a thrombin calibrator. Calibration curves corrected for effects of plasma colour, and allowed conversion of fluorescence levels (nonlinear if required) into nanomolar thrombin concentrations.[16] First-derivative thrombin generation curves provided levels of thrombin lag time (min), maximal thrombin concentration (nM), and thrombin capacity (area-under-the-curve = ETP in nM x min).[4] Samples in wells were pre-incubated with

modulating agents for 10 minutes at 37°C.

For whole-blood thrombin generation, citrated blood samples were thoroughly mixed with substrate solution (Z-GGR-AMC dissolved into BSA60 buffer) and trigger solution (1 pM TF, 6 mM $CaCl_2$ and 3 mM $MgCl_2$ dissolved into BSA5 buffer).[4] The volume ratio of blood, trigger solution and substrate solution was 3:2:1. A modified Excel-based template was used to obtain calibrated, first derivative thrombin generation curves.

Plasma thrombin pool assessment

To estimate thrombin pools, wells of round bottom 96-well plates were used without additional coating. Plasma samples were preincubated with Nb106 or vehicle buffer for 10 min at 37 °C, before measuring thrombin generation, which was commonly triggered with $CaCl_2$/$MgCl_2$, phospholipids and tissue factor.

For the assessment of prothrombin consumption, prothrombin levels were measured both before and after 60 min of tissue factor addition. Measurements were carried out in diluted subsamples using a molar excess of staphylocoagulase, *i.e.* a venom that exposes the catalytic site of prothrombin.[17] To reach a molar excess of staphylocoagulase, the overall plasma dilution was 1:400, as described.[18] Staphylocoagulase-activated prothrombin in the diluted samples was quantified using the chromogenic substrate S2238. Included were separate control samples with Nb106 added to the plasma prior to dilution. Note that the Nb106 concentration in the assayed diluted plasma samples was around 250 ng/mL.

Average thrombin lifetimes were calculated as the ratio of the total amount of thrombin generated during 60 minutes (ETP, nM·x min) to the amount of prothrombin consumed over the same period. This calculated lifetime hence represents the average duration during which thrombin remains proteolytically active over 60 minutes. This endpoint-based approach correlated well with reported kinetic lifetime values of antithrombin-deficient plasma, and allowed direct comparison with thrombin–antithrombin complex measurements. Average lifetimes of two reactive thrombin pools were calculated, assuming that pool 2 consisted of selectively displaced thrombin from fibrin by a saturating concentration of Nb106:

(1) $$\text{Fr. Pool 1} = \frac{\text{TC}_{\text{Nb106}}}{\text{TC}_{\text{Con}}}$$

(2) $$\text{Fr. Pool 2} = 1 - \frac{\text{TC}_{\text{Nb106}}}{\text{TC}_{\text{Con}}}$$

(3) $$\text{PC (Prothrombin consumption)} = \text{Prothrombin}_{\text{plasma}} - \text{Prothrombin}_{\text{serum}}$$

(4) $$\text{Lifetime in pool 1} = \frac{\text{TC}_{\text{Nb106}}}{\text{PC}_{\text{Nb106}}}$$

(5) $$\text{Lifetime in pool 2} = \frac{\frac{\text{TC}_{\text{Con}}}{\text{PC}_{\text{Con}}} - \text{lifetime in pool 1} \times \text{Fr. Pool 1}}{\text{Fr. Pool 2}}$$

Herein, "Fr. Pool 1" represents the thrombin capacity (TC) fraction of thrombin in pool 1, and "Fr. Pool 2" the fraction in pool 2.

Prothrombin clotting time

Normal pool plasma (NPP) was preincubated with Nb106 (100 µg/mL) or vehicle (control) for 10 min at 37°C. Clotting was triggered with 1-1000 pM TF, 4 µM procoagulant phospholipids, 11 mM $CaCl_2$ and 5.5 mM $MgCl_2$. Plasma clotting times were measured using a STart apparatus (Stago, Paris, France).

Clot turbidity assay

Fibrin-dependent turbidity changes in clotting plasma were monitored for 50 minutes in triplicate in 96-well plates, using spectrophotometric recording (SpectraMax, Molecular Devices, Salzburg, Austria) of the optical density at 405 nm.[19] For coagulation induction, samples of plasma from healthy subjects or patients were mixed with 1 pM TF, 4 µM procoagulant phospholipids, 11 mM $CaCl_2$ and 5.5 mM $MgCl_2$.

Plasma fibrinogen assessments

Active fibrinogen concentrations in plasmas were measured by the Clauss method by triggering with purified human thrombin.[9] Plasma levels of fibrinogen were measured by conventional immunoassay on a standard coagulometer. Levels were expressed as antigen levels (g/L) or as percentages of mean of controls of 3.0 g/L. For functional fibrinogen measurements (Claus method), reference values were 1.5-4.5 g/L, for fibrinogen antigen 2.4-3.6 g/L (80-120%).[20]

Clot contraction

To measure clot formation and contraction, samples of reconstituted PRP (platelet count: 200 × 10^9/L) preincubated with Nb106 (100 µg/mL) or vehicle (control) were triggered with 1 pM TF and 10 mM $CaCl_2$.[21] Clotting was monitored in 1 mL TH-CV-1000 glass tubes (SD Innovation, Frouard, France) at 37 °C, which were imaged for up to 150 minutes. The images were analysed for pixel surface-area-coverage (SAC%) of visible clots, using a home-made Fiji script.

Light transmission and confocal microscopy

Normal pool plasma (NPP) and antithrombin-III depleted plasmas were preincubated with Nb106 (100 µg/mL) or vehicle (control) for 10 minutes at 37 °C. Fibrin formation was then triggered with 1 pM TF, 4 µM phospholipids, 11 mM $CaCl_2$, and 5.5 mM $MgCl_2$. After thorough mixing, the mixture was immediately transferred to a glass slide and the fibrin formation was observed with an inverted light transmission microscope with 63x objective (Leica DFC 3000 G, Wetzlar, Germany). Confocal microscopy of fibrin structures was performed, as described elsewhere.[12]

Atomic force microscopy of single molecule and polymerized protofibrils

Atomic force microscopy (AFM) was employed for the imaging of fibrin protofibril and fibril assembly, as detailed previously. In brief, purified fibrinogen (0.5 mg/mL), $CaCl_2$ (2.5 mM) and Nb106 (100 µg/mL) or vehicle control solution were mixed to obtain 20 µL sample volumes. After addition of thrombin (10 nM), reactions were stopped in concatenated samples, with interval of 10 seconds, by addition of 1480 µL of Tris-buffered saline. Subsamples of 50 µL were deposited onto mica discs (pre-treated with 2 mM $NiCl_2$ for 10 minutes). For end-stage measurements, fibrinogen (final concentration 0.5 mg/mL), $CaCl_2$ (2.5 mM) and TBS buffer were pre-mixed in a final volume of 20 µL, and transferred to freshly cleaved mica discs (pre-treated with 2 mM $NiCl_2$ for 10 minutes). After adding thrombin (10 nM), the solution was spread on the disc surface. Samples were allowed to clot for 5 minutes. Before AFM imaging, discs were rinsed with dH_2O and dried under nitrogen gas. The fibrin samples were imaged with a Nanoscope IIIa MultiMode AFM (Veeco Instruments, Santa Barbara, CA, USA), operated in tapping mode. Image processing and analysis was using Nanoscope software (Veeco Instruments).

Peptides and aptamers for testing interference with thrombin

Based on established binding of thrombin to N-terminal regions of fibrin Aα and Bβ chains,[22]

two novel peptides were designed corresponding to these sites, which were synthesized (>95% purity) by Synpeptide (Nanjing, Jiangsu, China). The constructed 30 amino-acid peptide-1 (Pep1) consisted of residues 40-69 of the full-length product of wildtype human *FGA* (3.65 kDa). The 35 amino-acid peptide-2 (Pep2) consisted of residues 71-105 of the product of wildtype human *FGB* (3.78 kDa). Aptamer 1 of 4.88 kDa (blocking thrombin exosite I), aptamer 2 of 10.4 kDa (blocking thrombin exosite II), and aptamer 3 of 20.2 kDa (blocking thrombin exosites I and II) were used, as before.[4]

Thrombin-antithrombin complex assessment

Thrombin-antithrombin (TAT) complex levels were measured using a high-throughput enzyme-linked immunosorbent assay (ELISA), essentially as described.[23] In short, 384-well microliter plates were coated overnight at 4 °C with 2 µg/mL novel single domain antibody against antithrombin Nb1024, fused with an Fc-tail (Synapse Research Institute, Maastricht, The Netherlands), in carbonate-bicarbonate coating buffer pH 9.6. The wells were then blocked with phosphate-buffered saline pH 7.4 containing 20 mg/mL BSA and 0.05% Tween-20 for 2 hours at room temperature. After washing, activated plasma samples (diluted 1:20 in phosphate-buffered saline containing 10 mg/mL BSA) were added and incubated for 2 hours. Hereafter, the wells were incubated overnight with peroxidase-conjugated anti-prothrombin polyclonal antibody (1:10000 dilution; Affinity Biologicals, Ontario, Canada) for assessment of TAT levels. Plates were then washed with phosphate-buffered saline containing 0.05% Tween-20 before addition of SuperSignal West Femto Maximum Sensitivity substrate (ThermoFisher). Luminescence was measured with a Synergy H1 multimode microplate reader (Biotek, Bad Friedrichshall, Germany). Signals were converted into molar levels of TAT using a calibration curve of prothrombin.

Reactive thrombin lifetime for a given activated plasma sample was calculated from the 60-minutes thrombin capacity level (nM x min) from calibrated thrombin generation curves and the 60-minutes TAT concentration (nM) at the same activation conditions.

Ex vivo thrombus formation during whole blood flow

Whole-blood thrombus formation to observe platelet-dependent fibrin clotting under flow conditions (wall shear rate of 200 or 1000 s^{-1}) was assessed, basically as described for mouse blood[12] or for human blood.[13] In all cases, a transparent parallel-plate microfluidic chamber was used containing a coverslip with microspots of collagen-I.[24] Citrate-anticoagulated blood

samples were flowed over the surface upon continuous recalcification using a y-shaped dual inlet system, connected to two pulse-free perfusion pumps.[25] Optimal coagulation was obtained by co-infusion of the blood samples 10:1 (vol/vol) with recalcification medium (1 pM TF, 3.75 mM $MgCl_2$ and 7.5 mM $CaCl_2$). Blood samples were pre-incubated with control vehicle or with Nb106. as indicated.

For mouse flow studies, blood samples were prelabelled with Alexa Fluor-647 anti-glycoprotein IX antibody (clone 56F8) plus Alexa Fluor-488 fibrinogen.[12] Recording was with a Leica DMI 6000 B fluorescence microscope, equipped an 63x oil-immersion objective. The images were processed with an Instant Computational Clearing method to remove out-of-focus background blur.[12] For human flow studies, blood samples were prelabelled with Alexa Fluor-647 fibrinogen.[25] Recording was with an inverted EVOS fluorescence microscope, containing an Olympus 60x oil-immersion objective with high z-axis resolution and an 8-bit monochrome camera. Images were semi-automatically processed by scripts in the AForge. NET image processing library.[26]

Preparation of PPACK–thrombin complex

PPACK–thrombin was prepared by mixing human α-thrombin with PPACK at a 1:1 molar ratio. The reaction mixture was incubated for 30 minutes at room temperature. Unreacted PPACK was removed by chromatography using a desalting column (HiTrap desalting on Sephadex G-25 resin, 5 mL), pre-equilibrated with Hepes buffer pH 7.45. The concentration of PPACK–thrombin was determined spectrophotometrically at 280 nm using an extinction coefficient of 1.83.

To confirm complete inhibition of thrombin activity, 1 µL of the purified PPACK–thrombin mixture was diluted into 499 µL BSA 5 buffer. A total of 125 µL of the diluted sample was transferred to a 96-well microplate, followed by the addition of 25 µL of S-2238 substrate solution (600 nM). Absorbance changes at 405 nm were recorded to monitor thrombin activity. The absence of residual free PPACK was determined by incubating 2 µL of the purified PPACK–thrombin preparation with 20 µL of active thrombin (10 nM) and 478 µL of BSA 5 buffer. Then, 125 µL of the mixture was added to a 96-well microplate, followed by the addition of 25 µL S-2238 substrate solution. Again, changes in absorbance at 405 nm were measured.

Data analysis

Statistical analyses were performed with GraphPad Prism 9 (San Diego, CA, USA). Data are

presented as mean ± SD, unless indicated otherwise. For normally distributed datasets, unpaired two tailed Student's t tests were used. Multiple groups were compared using a one-way ANOVA (Kruskal-Wallis test) followed by post-hoc testing for multiple comparisons. Inter-group interactions were analysed using two-way ANOVA with Sidak's correction. In the absence of normality, a Mann–Whitney U test was used for comparisons between two groups. Values of $p < 0.05$ were considered as statistically significant.

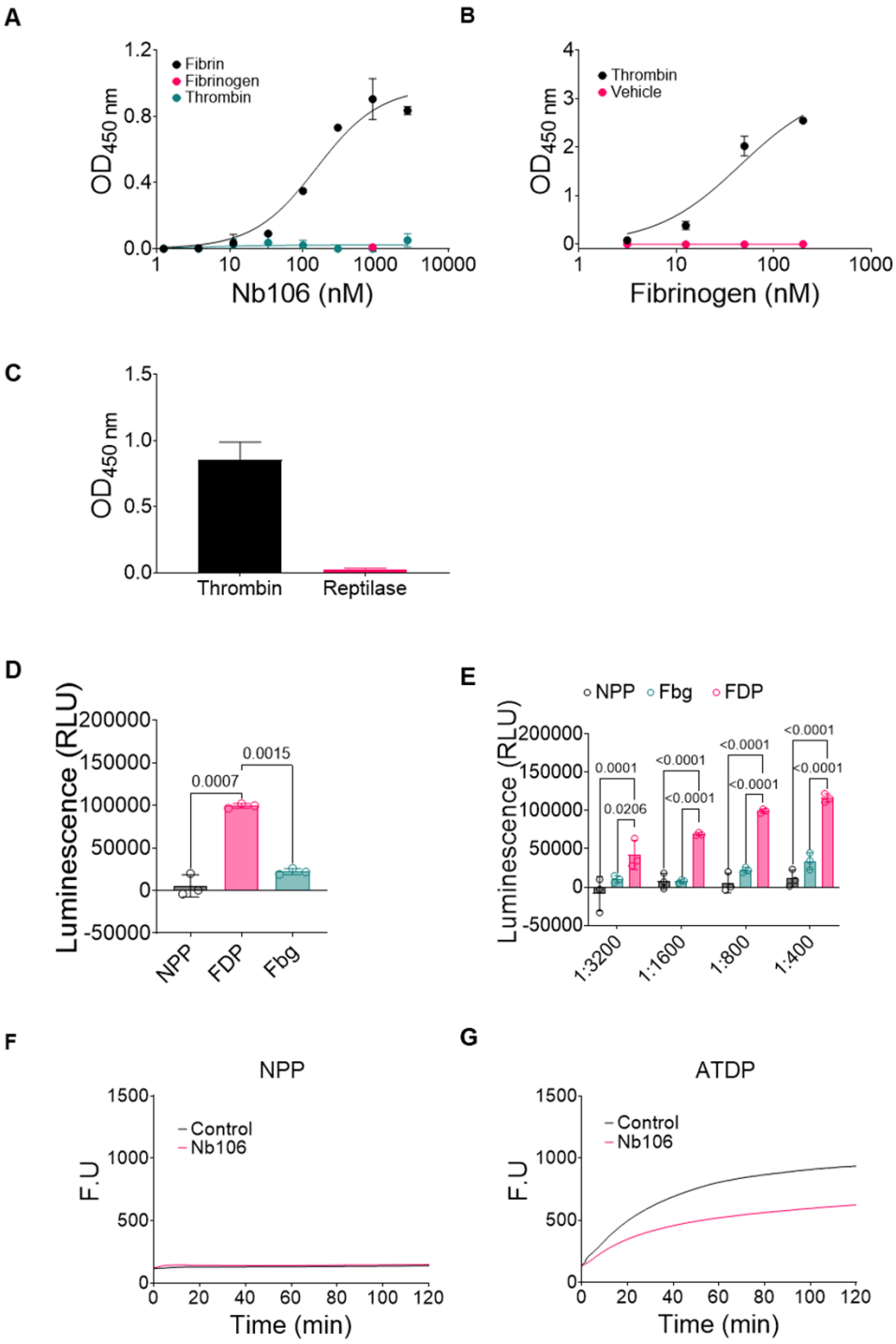

Suppl. Figure 1. Binding characterization studies of the selected single-chain antibody Nb106. (**A**) Nb106 binding to immobilized fibrin, but not fibrinogen or thrombin. In 96-wells, fibrinogen (10 µg/mL) plus thrombin (50 µg/mL) were coated overnight to form fibrin, while other wells contained only fibrinogen of thrombin. Plates were thoroughly washed with phosphate-buffered saline (PBS) containing 0.1% Tween-20 (PBS-T), and incubated with crude Myc-tagged single-chain antibodies for 1 hour. Antibody (Ab) binding was detected with 1 µg/mL mouse anti-c-Myc mAb (clone 9E10, purified in-house), followed by horse radish peroxidase (HRP)-labeled rabbit anti-mouse-Ab (1:1000, Daka, Santa Clara, CA, USA). Plates were stained with 3,3'5,5'-tetramethylbenzidine (Pierce, Appleton, WI, USA), with an acid stop

using 0.1 M H_2SO_4. Coloring was read at 450 nm. Results are shown for single chain c-Myc Nb106, which was selected from 10 clones with selective binding to immobilized fibrin only (total of 138 clones). (**B**) Binding of Nb106 to fibrin monomers. Wells were coated with anti-c-Myc Ab (1 µg/mL) in carbonate buffer, blocked with 2% skimmed milk in PBS for 1 hour, and incubated with purified Nb106 (5 µg/mL) in blocking buffer. After washing, the wells were incubated with fibrin monomers (thrombin) or fibrinogen (vehicle) at indicated concentrations. Fibrin monomers were made by incubating fibrinogen (200 nM) with thrombin (20 nM) and GPRP (200 µM) in blocking buffer. Serial dilutions of fibrin monomers were made in blocking buffer. After thorough washing and blocking with 2% albumin, fibrin monomers were detected in the presence of 200 µM GPRP. Detection was with rabbit anti-fibrinogen mAb (1:2000, Dako), followed by HRP-labeled swine-anti rabbit Ab. Plates were developed as described for panel A. Calculation showed an apparent KD for Nb106 46 nM, which is an underestimate due to the various washing steps. (**C**) Abolished Nb106 binding to fibrin formed by cleavage of only fibrinopeptide FpA. Wells were coated with anti-fibrinogen mAb (1:5000), blocked with 2% albumin, thoroughly washed, incubated with fibrinogen (300 µg/mL) for 1 hour, and washed again. Some wells were then incubated with thrombin (20 nM) or reptilase (25 µg/mL, cleaving FpA at Arg16-Gly17 but not FpB). After a wash, treatment with PPACK (50 µM) and another wash step, the wells were incubated with Nb106 (10 µg/mL), and stained as described for panel A. (**D-E**) Selective binding of Nb106 to plasmin-treated fibrin, but not fibrinogen. Coated Nb106 (10 µg/mL) was incubated with normal pool plasma (NPP), with plasma containing fibrin degradation products (FDP), or with purified fibrinogen (Fbg). (**D**) Paratope binding was detected via ELISA using an HRP-conjugated polyclonal anti-fibrinogen Ab. Shown are relative luminescence units(RLU), means of triplicates. (**E**) Paratope binding after incubation with indicated dilutions of NPP, FDP or Fbg. (**F-G**) Thrombin displacement from coated fibrin by Nb106. In-situ coated fibrin (50 µg/mL fibrinogen plus 20 nM thrombin, 30 minutes) in wells was washed, and post-incubated with NPP (**F**) or antithrombin-deficient plasma (ATDP) (**G**) in the presence of vehicle medium or Nb106 (100 µg/mL). Fluorescence from Z-GGR-AMC cleavage was measured over time (mean ± SD, n=3). Binding characterization studies of selected single-chain antibody Nb106.

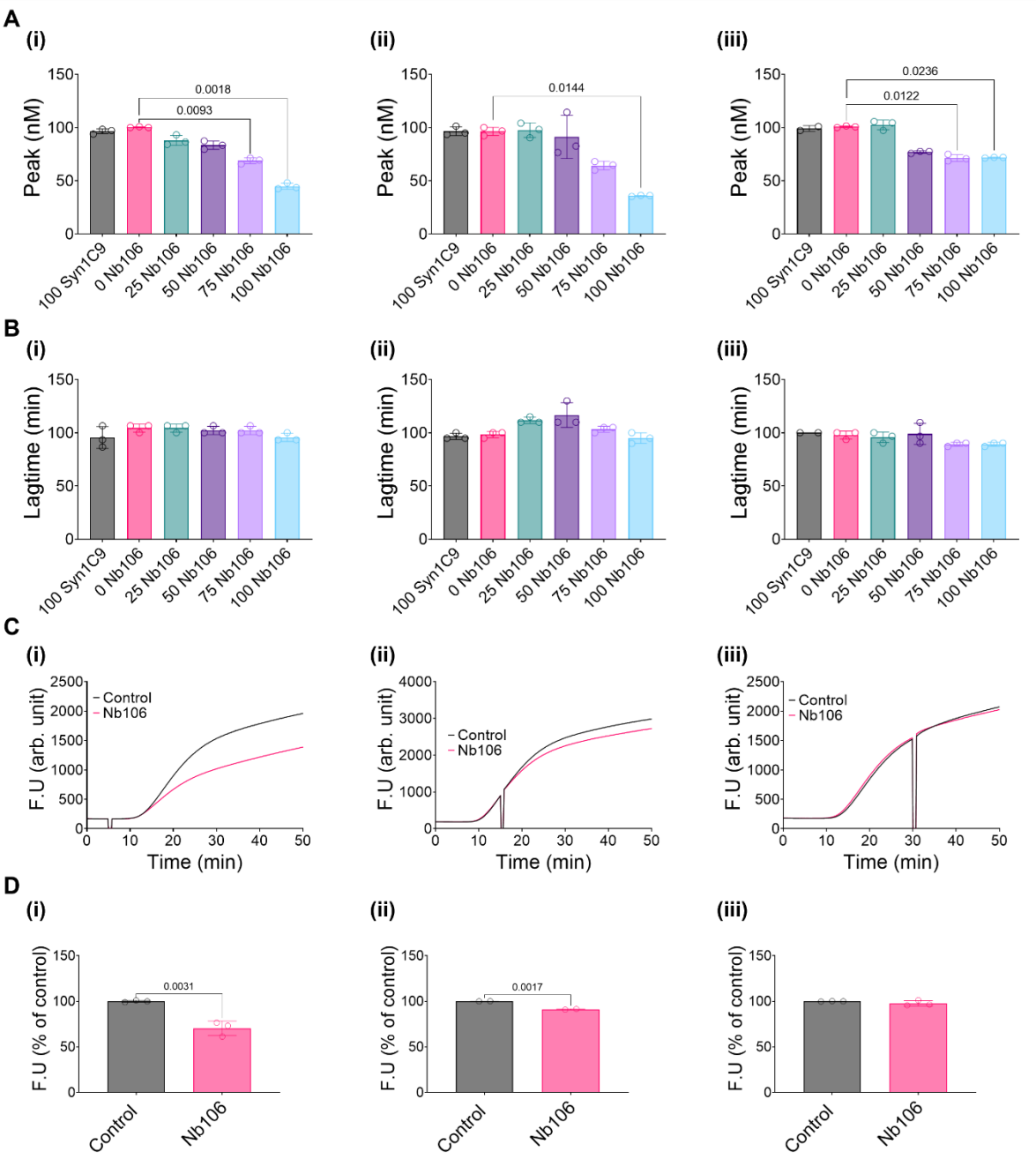

Suppl. Figure 2. Assessment of the anticoagulant potential of anti-fibrin Nb106.

(**A-B**) Parallel samples of plasma (**i**), PRP (**ii**) and whole blood (**iii**) were pre-incubated with vehicle control solution, Nb106 (25-100 µg/mL) or indifferent Nb-Syn1C9 (100 µg/mL). Coagulation was triggered with 1 pM TF, as in Figure 1. Shown are maximal thrombin levels (**A**) and lag times (**B**) relative to the control condition. Means ± SD (n=3), one-way ANOVA (non-parametric). (**C-D**) Plasma samples were triggered with 1 pM TF, and Nb106 (100 µg/mL) was added at 5 (**i**), 15 (**ii**) or 30 (**iii**) minutes. Shown are raw fluorescence curves of thrombin substrate cleavage (**C**), and normalized fluorescence values after 50 minutes (**D**). Mean ± SD (n=3), Mann-Whitney U-test. Note gradual decline of Nb106 inhibition over time. Note that Nb106 effect sizes were similar at 0.1 and 10 pM TF.

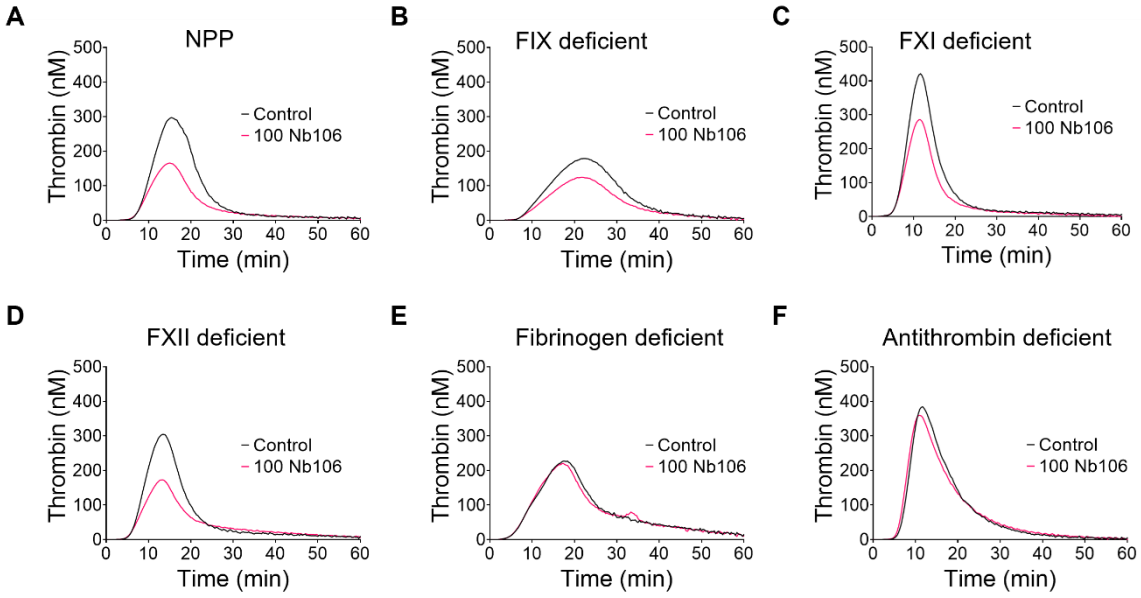

G

Plt + Plasma deficiency	Effect of Nb106 (control 100%)					
	Relative lagtime (%)	*P*	Relative peak (%)	*P*	Relative ETP (%)	*P*
None (NPP)	98 ± 2	*0.37*	56 ± 7	*0.001*	60 ± 1	*0.001*
Fibrinogen	99 ± 0.3	*0.42*	99 ± 0.3	*0.17*	98 ± 1	*0.14*
Factor IX	102 ± 2	*0.52*	69 ± 3	*<0.001*	70 ± 2	*0.001*
Factor XI	98 ± 3	*0.37*	68 ± 2	*<0.001*	69 ± 1	*<0.001*
Factor XII	101 ± 1	*0.37*	57 ± 3	*<0.001*	72 ± 3	*0.001*
Antithrombin	96 ± 3	*0.16*	95 ± 0.4	*0.08*	100 ± 1	*0.81*

Suppl. Figure 3. Thrombin-inhibiting effect of Nb106 in reconstituted PRP relying on plasma fibrinogen and antithrombin.

(**A-G**) Thrombin generation was triggered with TF using different plasma types after incubation with vehicle control solution or Nb106 (100 µg/mL). Plasma types were supplemented with platelets (2×10^8/mL) from three donors to obtain reconstituted PRP. Compared were normal pool plasma (NPP) (**A**), and plasmas deficient in factor IX (**B**), factor XI (**C**), factor XII (**D**), fibrinogen (**E**), or antithrombin (**F**). Shown are representative curves and quantified curve parameters thrombin lag time, maximum and capacity (ETP), with statistics (**G**). Mean ± SD (n=3-5), two-way ANOVA, non-parametric.

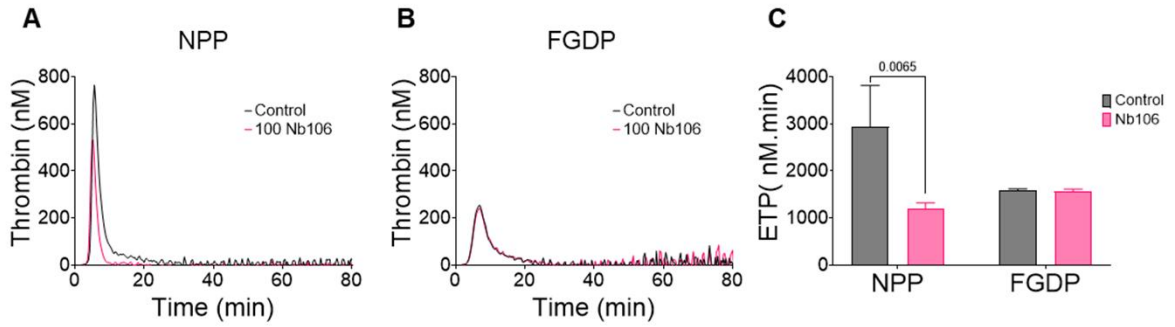

Suppl. Figure 4. Thrombin-inhibiting effect of Nb106 upon triggering with kaolin. (**A-C**) Thrombin generation was triggered in normal pool plasma (NPP) (**A**) or fibrinogen-deficient plasma (FGDP) (**B**) with $CaCl_2$/$MgCl_2$ and phospholipids plus 5 µg/mL kaolin, as in aPTT. Preincubation was with vehicle solution (control) or 100 µg/mL Nb106. (**C**) Quantification of thrombin capacity (ETP). Mean ± SD (n=3 experiments), two-way ANOVA, non-parametric).

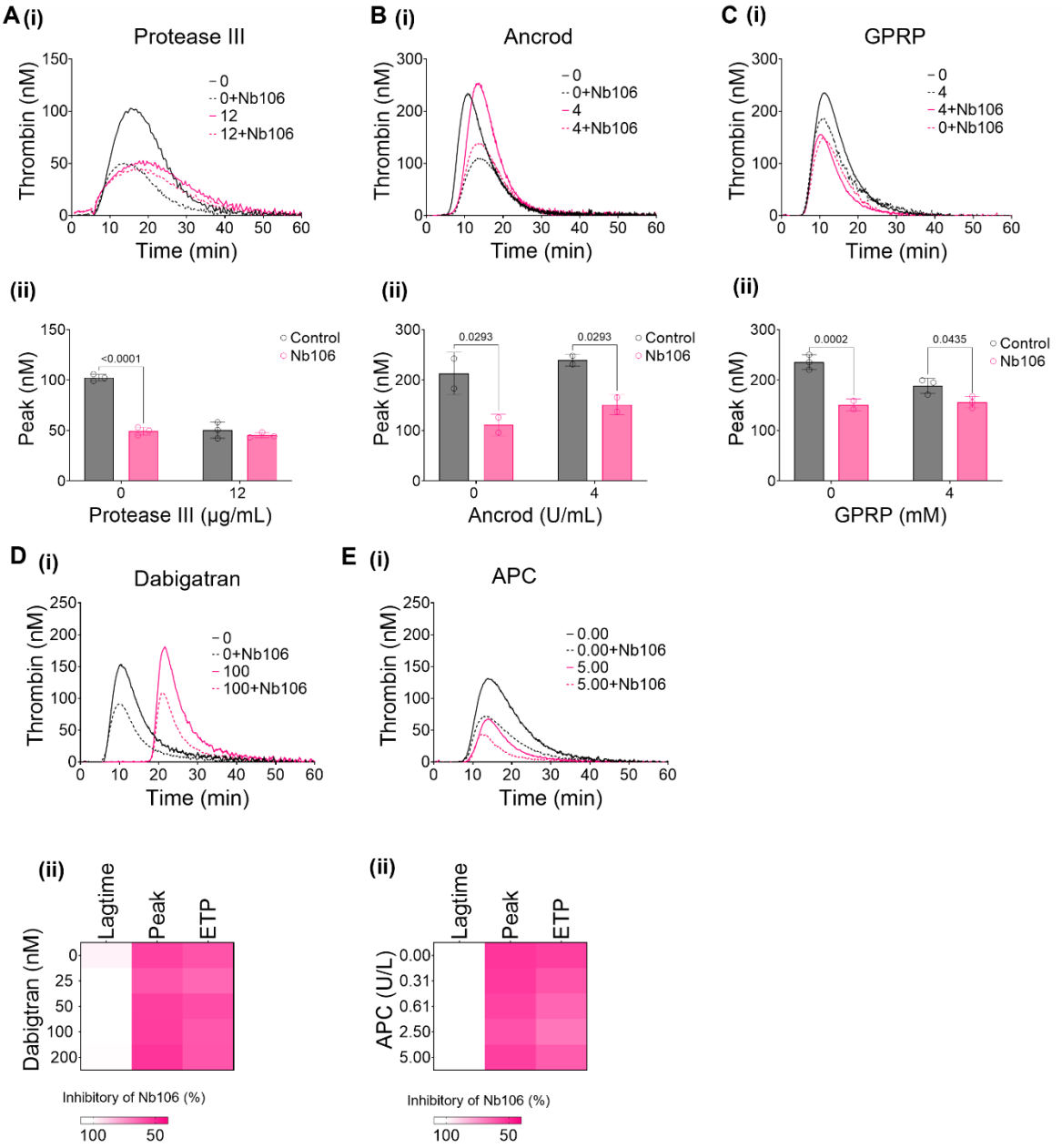

Suppl. Figure 5. Effects of fibrinogen degradation and coagulation interference on Nb106 inhibition.

(**A-C**) Normal pool plasma was preincubated with vehicle, 12 µg/mL protease III (**A**), 4 units/mL protease ancrod (**B**) or 4 mM GPRP (**C**). Coagulation was triggered with TF in the absence or presence of Nb106 (100 µg/mL), as in Figure 1. Shown are representative thrombin generation curves (**i**), and maximal thrombin levels (**ii**). Mean ± SD (n=3 experiments), two-way ANOVA (non-parametric). (**D-E**) Plasma samples were preincubated with 100 nM dabigatran (**D**) or 2.5 nM activated protein C (APC) (**E**). Representative traces of thrombin generation (**i**) and heat-mapped normalized values of curve parameters (**ii**). Mean results from triplicate experiments. Colour bar indicates inhibitory effect of Nb106 versus corresponding control condition.

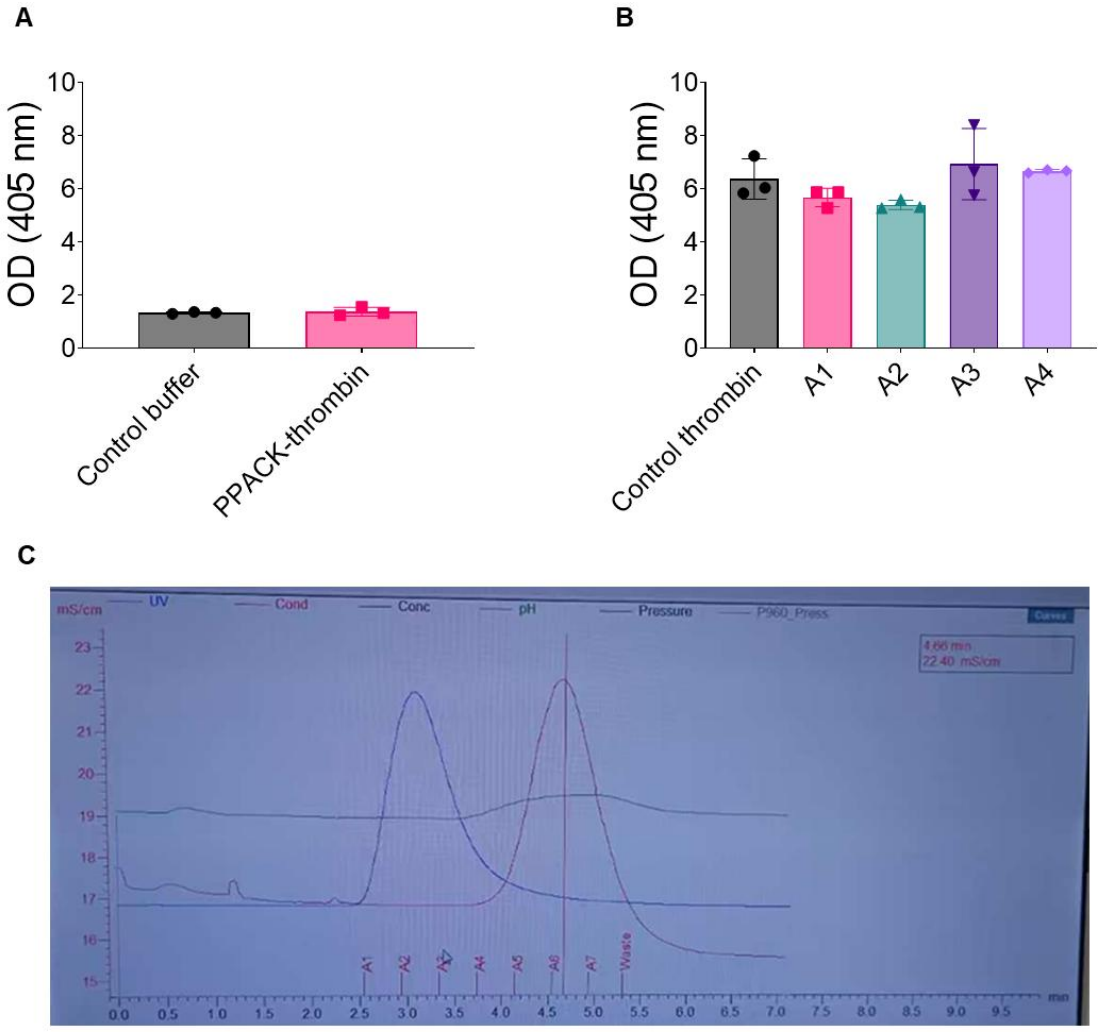

Suppl. Figure 6. Purification of PPACK–thrombin and activity testing of free thrombin and free PPACK.

(**A**) Activity testing of residual free thrombin. Thrombin activity was assessed by chromogenic substrate S2238 cleavage at 405 nm. PPACK–thrombin showed no detectable residual thrombin activity compared with control buffer. Mean ± SD (n=3 experiments), one-way ANOVA (non-parametric). (**B**) Residual free PPACK activity after desalting. Following purification on a desalting column, fractions A1–A4 were tested for free PPACK activity using chromogenic substrate S2238 at 405 nm. No residual free PPACK activity was detected in any fraction compared with control thrombin. Mean ± SD (n=3 experiments), one-way ANOVA (non-parametric). (**C**) Chromatographic profile of PPACK–thrombin purification. Representative chromatogram from desalting column purification. Fractions A1–A4 correspond to the main elution peak collected for further analysis.

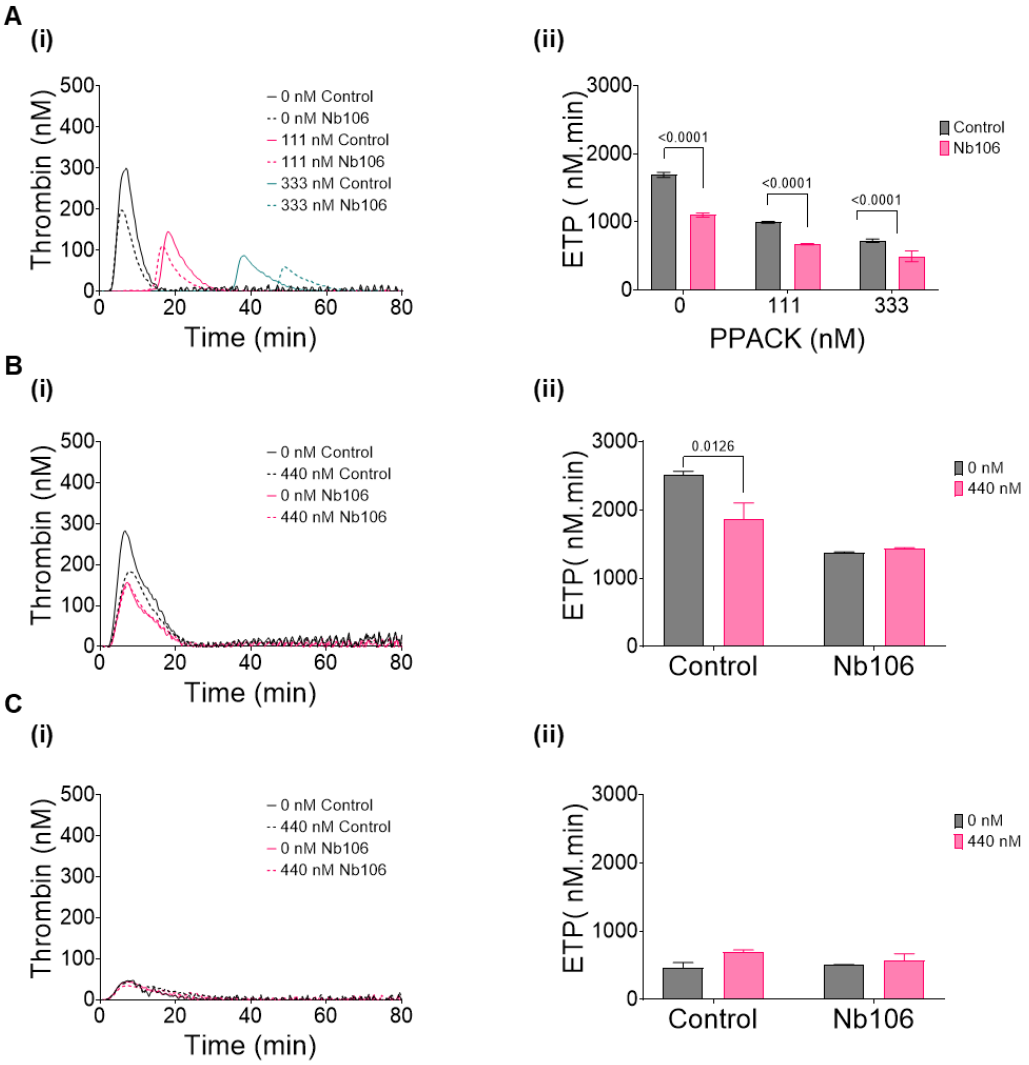

Suppl. Figure 7. Similar effects of PPACK-thrombin and Nb106 but not PPACK on thrombin generation.

(**A**) Consistent Nb106 effect on thrombin generation in the presence of PPACK. Thrombin generation in normal pool plasma was triggered as in Figure 1 with 1 pM TF in the absence or presence of Nb106 (100 µg/mL). Plasma samples were preincubated with indicated concentrations of PPACK (0, 111 and 333 nM). (**B-C**) Effects of PPACK-inactivated thrombin and Nb106 on thrombin generation. Thrombin generation in normal pool plasma (NPP) (**B**) or in fibrinogen-deficient plasma (FDP) (**C**) was triggered with 1 pM TF. Plasma samples were preincubated with vehicle (control), purified PPACK-thrombin (440 nM) and/or Nb106 (100 µg/mL). Mean ± SD (n=3 experiments), two-way ANOVA (non-parametric).

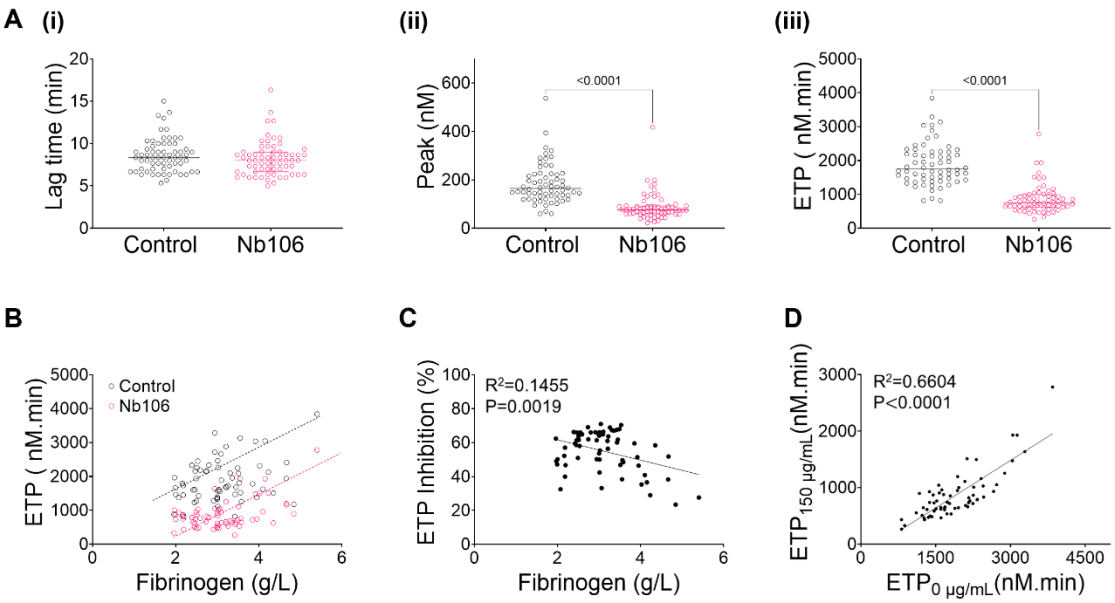

Suppl. Figure 8. Fibrin-dependent thrombin generation in cohort of healthy subjects.
Plasma samples from 64 healthy subjects were in part pre-incubated with Nb106 (150 µg/mL). TF-induced thrombin generation was assessed, as in Figure 1. (**A**) Indicated are per subject Nb106-mediated changes in thrombin lag time (**i**), maximal thrombin (**ii**) and thrombin capacity (ETP) levels (**iii**). Furthermore, (**B**) plots of plasma fibrinogen (Claus method) and thrombin capacity with(out) Nb106. Shown are conditions of control and Nb106 (n=64), p values in italic (Mann-Whitney U-test). (**C**) Effect of Nb106 on thrombin capacity, and (**D**) correlation of thrombin capacity levels with or without Nb106.

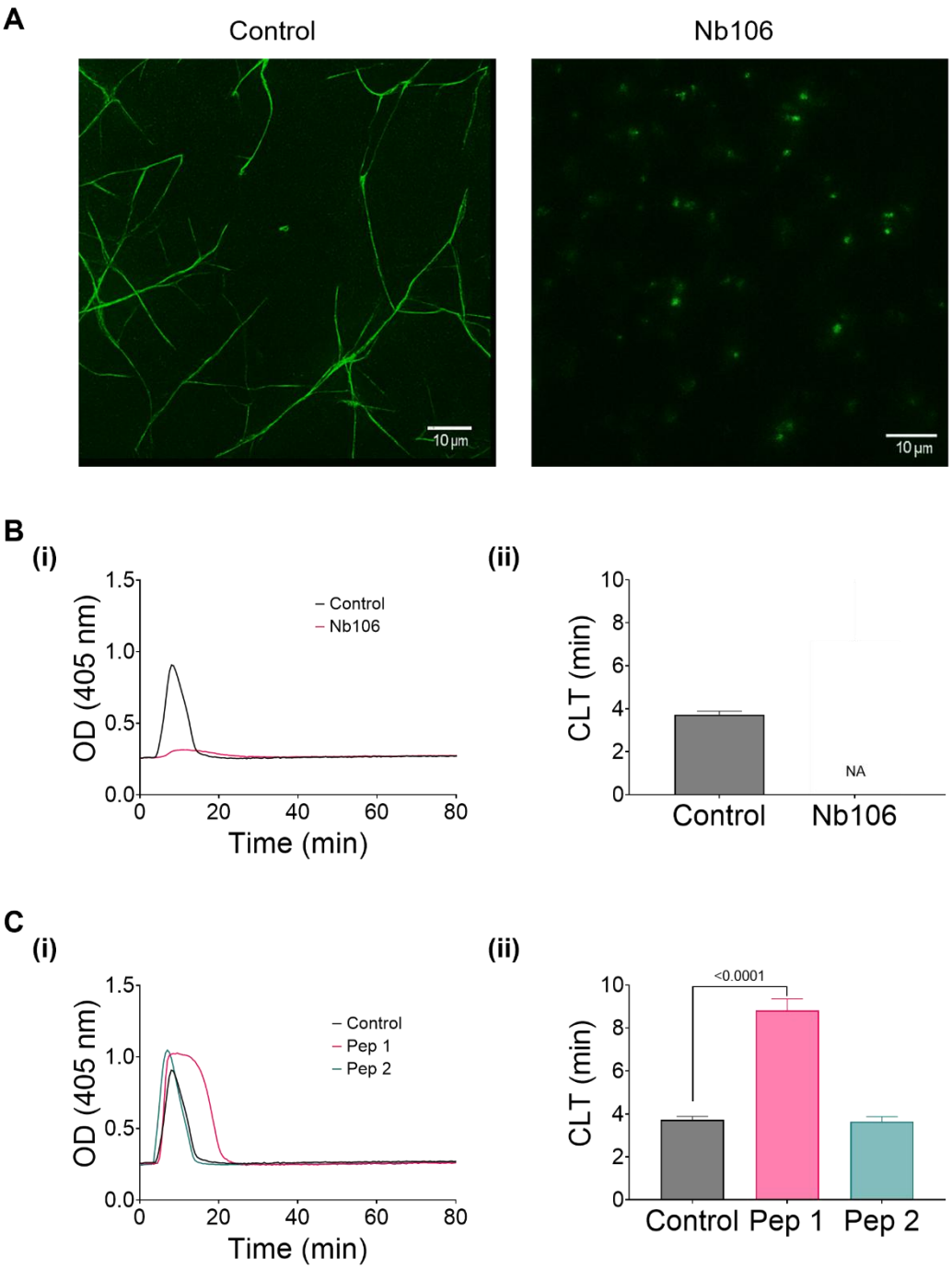

Suppl. Figure 9. Nb106 effects on clot lysis and on fibrin network formation.

(**A**) Representative confocal fluorescence microscopy images of fibrin structures from tissue-factor triggered plasmas in the absence (left) or presence (right) of Nb106 (100 µg/mL). Fibrin was formed from labeled Alexa Fluor-488 fibrinogen (green). Scale bar=10 µm. (**B-C**) Normal plasma containing tPA (3 nM) was triggered with $CaCl_2$/$MgCl_2$, phospholipids and 1 pM TF. Changes in optical density at 405 nm were followed at 37 °C to measure clot formation and subsequent lysis. (**B**) Plasma samples containing vehicle control medium or Nb106 (100 µg/mL). (**C**) Parallel samples contained Pep1 (500 µM) or Pep2 (500 µM), as indicated. Optical density traces are presentative for 3 experiments. Mean ± SD, one-way ANOVA (non-parametric).

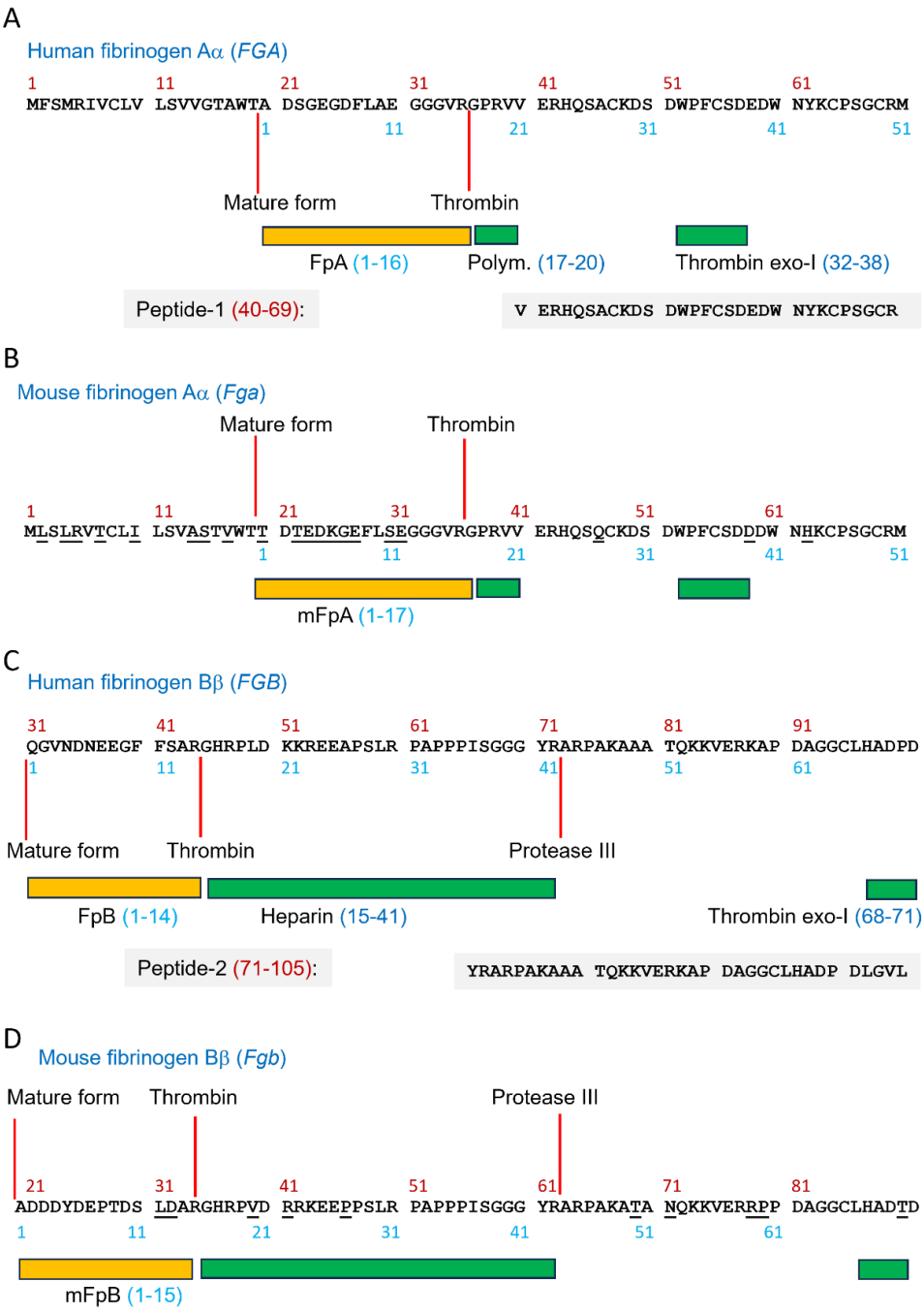

Suppl. Figure 10. Primary structure of N-terminal fibrin Aα and Bβ chains and the derived peptides.

(**A-B**) Primary amino acid sequence of human (UniProtKB P02671) and mouse (E9PV24) N-terminal parts of fibrinogen α-chains. Indicated are cleavage sites by maturation and thrombin. Numbering in red is according to corresponding transcripts, in blue according to the mature proteins. Indicated are the sequence of cleaved FpA peptide, of fibrin polymerization site and of postulated thrombin binding site via exosite-I.[22] Underlined are the non-conserved amino acid residues in the mouse protein. (**C-D**) Idem for the human (P02675) and mouse (Q8K0E8) N-terminal parts of fibrinogen β-chains. Indicated are cleavage sites by maturation, thrombin and protease III. Furthermore, sequences of cleaved FpB peptide, of heparin-platelet binding domain[27], and of postulated thrombin binding site via exosite-I.[22]

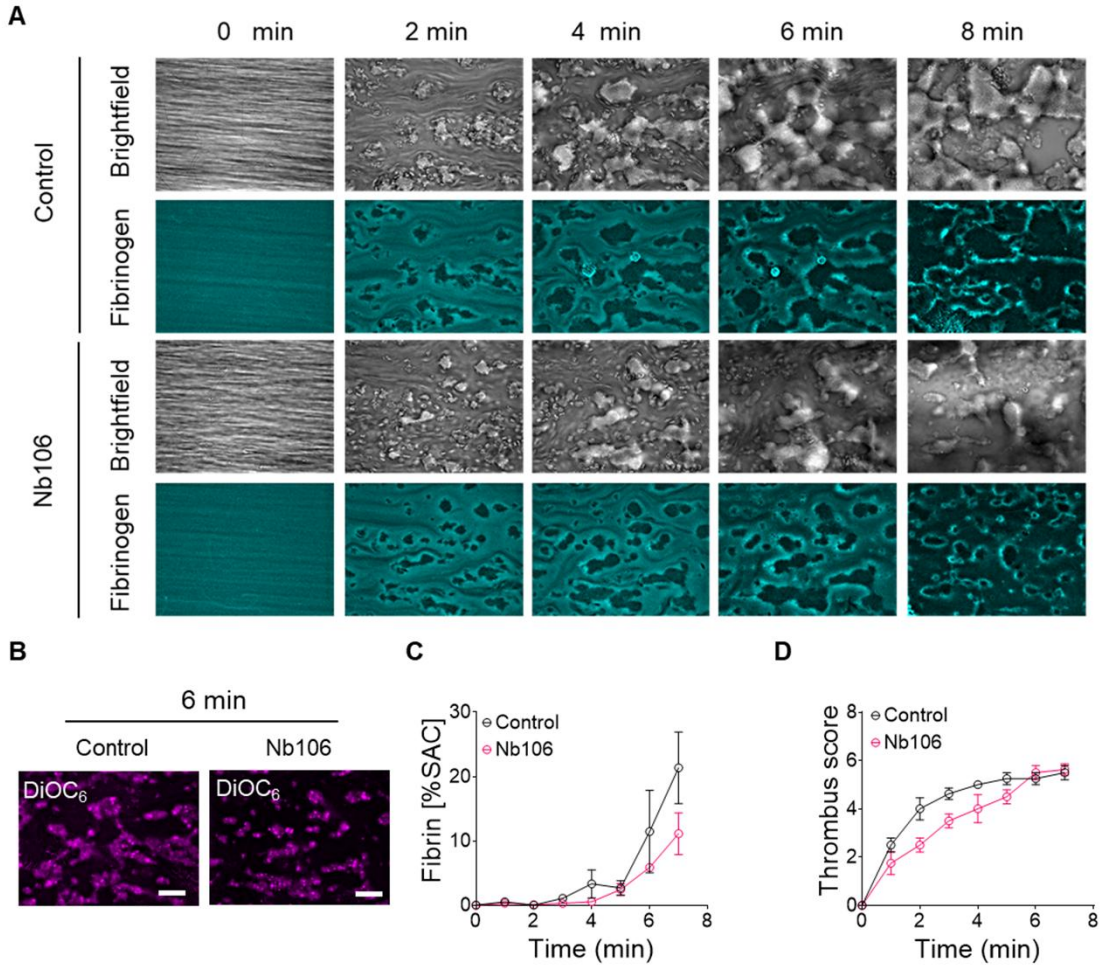

Suppl. Figure 11. Unaltered murine thrombus formation at high shear rate of 1000 s^{-1}.
(**A-B**) Citrated mouse blood was supplemented with Alexa Fluor 488-fibrinogen (green) and Alexa Fluor 647-anti-GPIX mAb (purple), with Nb106 (100 µg/mL) present as indicated. Blood samples were continuously recalcified with 1 pM TF, while perfusing over collagen-I microspots at high, arterial shear rate of 1000 s^{-1}. (**A**) Representative brightfield and fluorescence images of platelet-fibrin thrombi during flow. (**B**) Representative images of 6-minutes platelet deposition (AF647-αGPIX). Bars = 20 µm. (**C**) Quantification of fibrin surface area coverage and (**D**) thrombus score on scale 1-6 over time. Mean ± SD (n=4), two-way ANOVA. Note that fluorescence detection threshold was set above the background level of dissolved AF647-fibrinogen, to capture only increased levels of polymerized fibrin fluorescence.

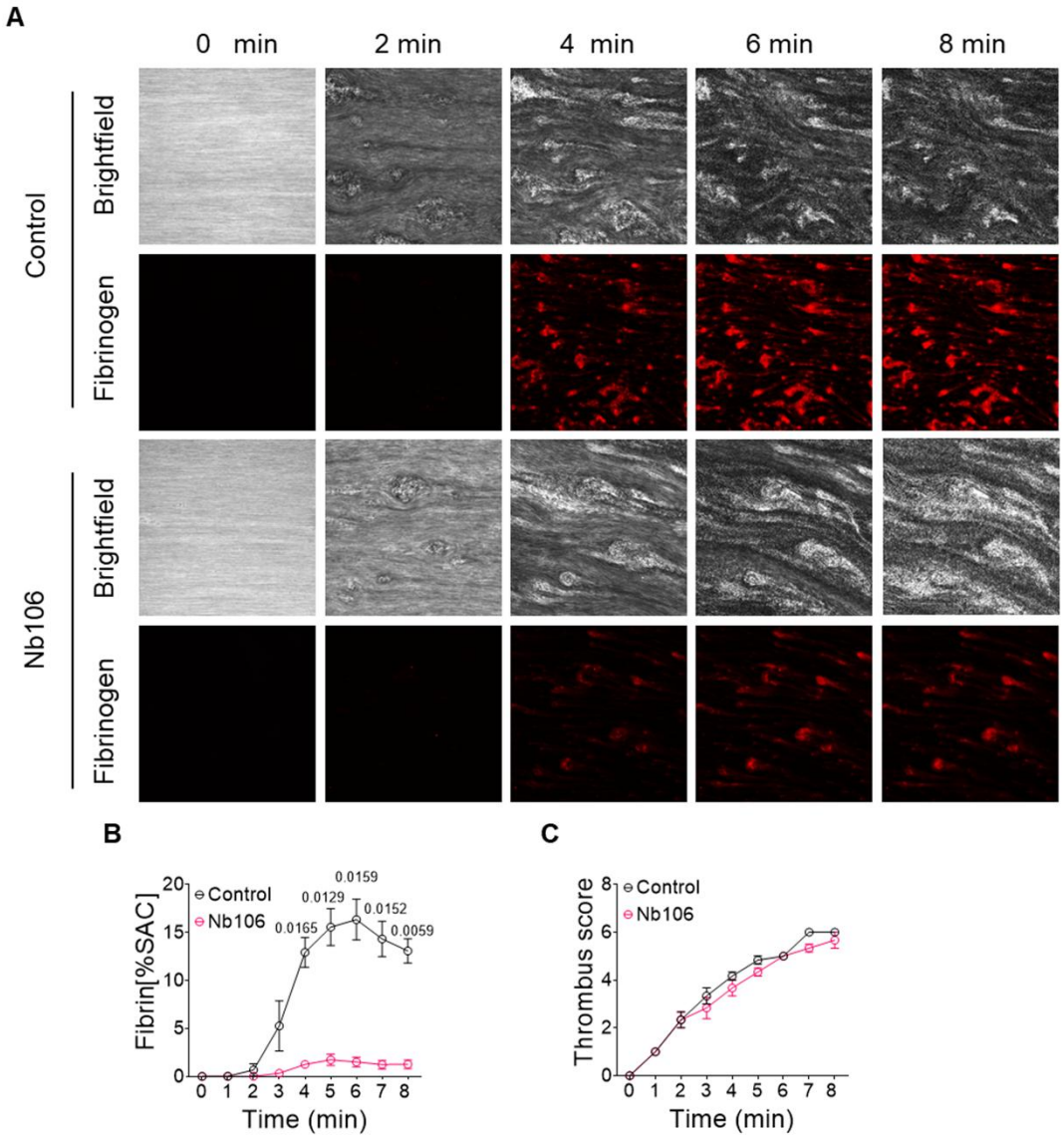

Suppl. Figure 12. Suppression by Nb106 of human thrombus formation limited to low shear rate of 200 s^{-1}.

(**A-C**) Citrated human blood samples were supplemented with Alexa Fluor 647-fibrinogen and with vehicle medium or Nb106 (100 µg/mL), as indicated. Blood perfusion was under continuous recalcification with 1 pM TF over collagen-I microspots at wall-shear rate of 200 s^{-1}.[25] (**A**) Representative brightfield and fluorescence images of fibrin-containing thrombi during flow in the absence or presence of Nb106. (**B**) Quantification of fibrin surface area coverage over time. (**C**) Quantification of thrombus score. Mean ± SD (n=4), two-way ANOVA.

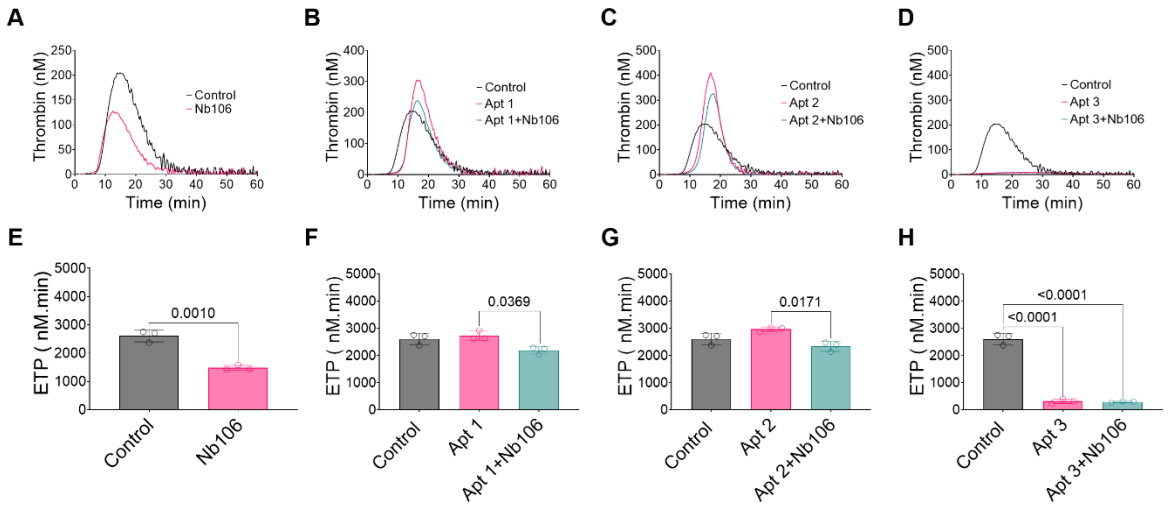

Suppl. Figure 13. Procoagulant effect of thrombin exosite-I or exosite-II inhibition.

To achieve thrombin exosite-I, exosite-II or combined exosite-I+II inhibition, plasma samples from healthy subjects were incubated with 5.3 μM Apt1, Apt2 or Apt3, respectively. TF-induced (1 pM) thrombin generation was measured in the absence or presence of Nb106 (100 μg/mL). Representative curves show effect of Nb106 alone (**A**), of Apt1 (**B**), Apt2 (**C**) or Apt3 (**D**). Furthermore , quantified maximal thrombin levels at these conditions (**E-H**). Mean ± SD (n=3).

References

1. Miszta A, Pelkmans L, Lindhout T, et al. Thrombin-dependent incorporation of von Willebrand factor into a fibrin network. *J Biol Chem*. 2014;289:35979–35986.
2. Wan J, Konings J, Yan Q, et al. A novel assay for studying the involvement of blood cells in whole blood thrombin generation. *J Thromb Haemost*. 2020;18:1291–1301.
3. Kremers RM, Kleinegris MC, Ninivaggi M, et al. Decreased prothrombin conversion and reduced thrombin inactivation explain rebalanced thrombin generation in liver cirrhosis. *PLoS One*. 2017;12:e0177020.
4. Sun S, Campello E, Zou J, et al. Crucial roles of red blood cells and platelets in whole blood thrombin generation. *Blood Adv*. 2023;7:6717–6731.
5. Macrae FL, Swieringa F, Heemskerk JW, Ariens RA. High fibrinogen γ' levels in patient plasma increase clot formation at arterial and venous shear rate. *Blood Adv*. 2021;5:3468–3477.
6. De Maat S, van Dooremalen S, de Groot PG, Maas C. A nanobody-based method for tracking factor XII activation in plasma. *Thromb Haemost*. 2013;110:458–468.
7. Wohner N, Sebastian S, Muczynski V, et al. Osteoprotegerin modulates platelet adhesion to von Willebrand factor during release from endothelial cells. *J Thromb Haemost*. 2022;20:755–766.
8. Marchi R, Vilar R, Durual S, et al. Fibrin clot properties to assess the bleeding phenotype in unrelated patients with hypodysfibrinogenemia due to novel fibrinogen mutations. *Thromb Res*. 2021;197:56–64.
9. Marchi R, Neerman-Arbez M, Gay V, et al. Comparison of different activators of coagulation by turbidity analysis of hereditary dysfibrinogenemia and controls. *Blood Coagul Fibrinolysis*. 2021;32:108–114.
10. Vanschoonbeek K, Feijge MA, van Kampen RJ, et al. Initiating and potentiating role of platelets in tissue factor-induced thrombin generation in the presence of plasma: subject-dependent variation in thrombogram characteristics. *J Thromb Haemost*. 2004;2:476–484.
11. De Laat B, Stragier H, de Laat-Kremers R, et al. Population-wide persistent hemostatic changes after vaccination with ChAdOx1-S. *Front Cardiovasc Med*. 2022;9:966028.
12. Beck S, Öftering P, Li R, et al. Platelet glycoprotein V spatio-temporally controls fibrin formation. *Nat Cardiovasc Res*. 2023;2:368–382.

13. Brouns S, van Geffen JP, Campello E, et al. Platelet-primed interactions of coagulation and anticoagulation pathways in flow-dependent thrombus formation. *Sci Rep*. 2020; 10:11910.
14. Mattheij NJ, Braun A, van Kruchten R, et al. Survival protein anoctamin-6 controls multiple platelet responses including phospholipid scrambling, swelling, and protein cleavage. *FASEB J*. 2016;30:727–737.
15. Al Dieri R, de Laat B, Hemker HC. Thrombin generation: what have we learned? *Blood Rev*. 2012;26:197–203.
16. Hemker HC, Giesen P, Al Dieri R, et al. Calibrated automated thrombin generation measurement in clotting plasma. *Pathophysiol Haemost Thromb*. 2003;33:4–15.
17. Kessels H, Willems G, Hemker HC. Analysis of thrombin generation in plasma. *Comput Biol Med*. 1994;24:277–288.
18. de Laat-Kremers RMW, Yan Q, Ninivaggi M, de Maat M, de Laat B. Deciphering the coagulation profile through the dynamics of thrombin activity. *Sci Rep*. 2020;10:12544.
19. Longstaff C. Measuring fibrinolysis: from research to routine diagnostic assays. *J Thromb Haemost*. 2018;16:652–662.
20. Campello E, Marobin M, Barbot M, et al. The haemostatic system in acromegaly: a single-centre case-control study. *J Endocrinol Invest*. 2020;43:1009–1018.
21. Aleman MM, Byrnes JR, Wang JG, et al. Factor XIII activity mediates red blood cell retention in venous thrombi. *J Clin Invest*. 2014;124:3590–3600.
22. Pechik I, Madrazo J, Mosesson MW, Hernandez I, Gilliland GL, Medved L. Crystal structure of the complex between thrombin and the central E region of fibrin. *Proc Natl Acad Sci USA*. 2004;101:2718–2723.
23. Willems RA, Konings J, Huskens D, et al. Altered whole blood thrombin generation and hyperresponsive platelets in patients with pancreatic cancer. *J Thromb Haemost*. 2024;22:1132–1144.
24. De Witt SM, Swieringa F, Cavill R, et al. Identification of platelet function defects by multi-parameter assessment of thrombus formation. *Nat Commun*. 2014;5:4257.
25. Navarro S, Stegner D, Nieswandt B, Heemskerk JW, Kuijpers ME. Temporal roles of platelet and coagulation pathways in collagen and tissue factor induced thrombus formation. *Int J Mol Sci*. 2021;23:358.

26. Herfs L, Swieringa F, Jooss N, et al. Multiparameter microfluidics assay of thrombus formation reveals increased sensitivity to contraction and antiplatelet agents at physiological temperature. *Thromb Res*. 2021;203:46–56.
27. Mosesson MW. Fibrinogen and fibrin structure and functions. *J Thromb Haemost*. 2005;3:1894–1904.